

Supporting Information

Supporting Methods.....	1
Supporting Results	2
References Cited.....	3
Supporting Tables.....	4
Supporting Figures	19

Supporting Methods

Genetree analysis. We revisited the coalescent analysis of Gómez-Alpizar *et al.* (1) using their data and ours to investigate the sensitivity of root inference to estimates of migration rates. Our concern was that there is little power to estimate migration rates with only a single locus, yet these rates were used to infer the rooting of structured coalescent trees in the program Genetree (2). Furthermore, Gómez-Alpizar *et al.* considered migration to and from South America, which confounds migration from Mexico and other global populations. *P. infestans* is transported transcontinentally and intercontinentally via infected seed tubers, and there is a vibrant commercial seed tuber trade from Northwest Europe with known pathways of migration from Europe to South America.

We revised the Genetree analysis of the P3 and P4 mtDNA regions using sequences from Gómez-Alpizar *et al.* (1) for isolates from Mexico and the Andes but removing the haplotypes representing the *P. andina* isolates (haplotype 1c). The topology and rooting of the coalescent tree for the *P. infestans* haplotypes remained the same. We inferred the maximum likelihood value of theta and a symmetric migration rate for the revised data set. We then used 1×10^7 simulations to examine the inferred subpopulation of the most common recent ancestor (MRCA) of the sample while varying theta and symmetric migration rates using three sets of runs, each set using a different starting seed.

For the RAS nuclear gene, we repeated the Gómez-Alpizar *et al.* (1) analysis while varying migration rates. We used their data set and value of theta. We conducted two runs of 1×10^7 simulations for each set of migration rates. We varied migration rates from low and symmetric to the values used by Gómez-Alpizar *et al.* We also examined the coalescent history of the RAS locus using our sequences from Mexico and the Andes. The tree was rooted using ancestral states obtained from *P. ipomoeae*, *P. mirabilis*, and *P. phaseoli*. We used four runs of 1×10^6 or 1×10^7 simulations and three symmetric migration rates using two different values of theta (1.5 and 2.0) and four starting seeds.

Migration scenarios from SSR genotypes. The program Migrate version 3.3 was used to examine recent migration between the Andes and Mexico, using SSR genotypes. Three migration models were compared (3): bidirectional migration, migration from Mexico to the Andes only, and migration from the Andes to Mexico only. The runs used Brownian motion approximation for the stepwise mutation model, initial parameter values from FST, and mutation rates per locus estimated from the data. Bayesian inference across 10 replicates used slice sampling, uniform prior distributions from 0 to 1000 for both theta and M parameters, and four chains (temperatures: 1,000,000, 3.0, 1.5, 1.0) in which the cold chain was sampled at 10,000

steps at 200 step increments after a burnin of 500,000 steps. Models were evaluated using Bezier approximation of log marginal maximum likelihoods.

Supporting Results

Dependence of Genetree results on migration rates. When we removed *P. andina* from the Gómez-Alpizar *et al.* mitochondrial data set and included only the Mexican and South American isolates, the root location was uncertain such that there was equal probability of rooting in Mexico or South America when migration rates were symmetric (Table S7A). Asymmetric migration rates increased the probability of the root in the population that was the source of migration to around 0.95, irrespective of which population was assigned the higher emigration rate.

For the RAS locus, the location of the coalescent root was dependent on migration rates as well (Table S7B). When we used the Gómez-Alpizar *et al.* data under low symmetric migration rates the rooting was uncertain, and asymmetric migration rates affected the inferred population of origin. The migration rates used by Gómez-Alpizar *et al.* produced a high probability for a South American root, which replicates their result. The opposite condition produced a similarly high probability for a non-South American root. Therefore, both mitochondrial and RAS analyses were highly dependent on choice of migration parameters.

We used our data set to examine the root location of RAS for Mexican and Andean isolates only. Using RAS sequences from *P. andina*, *P. mirabilis*, *P. ipomoeae*, and *P. phaseoli*, we were able to unambiguously assign ancestral states to each segregating site and these ancestral states were used to root the *P. infestans* RAS tree. The coalescent history of the gene was simulated on the rooted topology to infer the location of the root in Mexico or the Andes. Moderate and inconclusive probabilities for root location were observed under nearly all conditions examined, including three symmetric migration rates and two values of theta (Table S8).

Key to the Gómez-Alpizar *et al.* analysis was their finding of a higher migration rate from South America to non-South American populations (i.e. Mexico, USA, and Ireland) than vice-versa using the nuclear RAS locus. Given this result, we used our SSR data to test among models of migration between the Andes and Mexico using the program Migrate (3). Multiple loci are expected to provide more robust estimates of migration rates for the nuclear genome than can be obtained from a single locus. This analysis revealed a higher migration rate from Mexico to the Andes than from the Andes to Mexico ($M = 11.7$ vs. 0.3 , respectively). Bayesian comparison of migration models strongly supported unidirectional migration from Mexico to the Andes (Bezier approximation of the log marginal likelihood = -11,055) compared to the opposite scenario of migration from the Andes to Mexico (-12,243) or bidirectional migration (-52,357). This result is consistent with the known directions of trade in commercial seed tubers.

References Cited

1. Gómez-Alpizar L, Carbone I, & Ristaino JB (2007) An Andean origin of *Phytophthora infestans* inferred from mitochondrial and nuclear gene genealogies. *Proc Natl Acad Sci U S A* 104(9):3306-3311.
2. Griffiths RC & Tavaré S (1994) Ancestral inference in population genetics. *Statistical science* 9(3):307-319.
3. Beerli P & Palczewski M (2010) Unified framework to evaluate panmixia and migration direction among multiple sampling locations. *Genetics* 185(1):313-U463.
4. Nei M (1987) *Molecular Evolutionary Genetics* (Columbia University Press, New York) p 512
5. Watterson GA (1975) On the number of segregating sites in genetic models without recombination. *Theoretical Population Biology* 7:256-276.
6. Tajima F (1989) Statistical method for testing the neutral mutation hypothesis by DNA polymorphism. *Genetics* 123(3):585-595.
7. Fu Y-X & Li W-H (1993) Statistical tests of neutrality of mutations. *Genetics* 133(3):693-709.

Supporting Tables

Table S1. Isolates used in the study.

ID	Original name	Year sampled	Country	State	Host	Source ¹	Lineage
<i>P. infestans</i>							
PiCO01	1011		Colombia	Cundinamarca	<i>S. tuberosum</i>	Restrepo	EC-1
PiCO02	1063		Colombia	Cundinamarca	<i>S. tuberosum</i>	Restrepo	EC-1
PiCO03	1064		Colombia	Cundinamarca	<i>S. tuberosum</i>	Restrepo	EC-1
PiCO04	1068		Colombia	Cundinamarca	<i>S. tuberosum</i>	Restrepo	EC-1
PiCO05	4084		Colombia	Cundinamarca	<i>Physalis peruviana</i>	Restrepo	US-8
PiEC01	EC_3843	2004	Ecuador		potato	Forbes	EC-1
PiEC02	EC_3527	2002	Ecuador		<i>S. andeanum</i>	Forbes	EC-1
PiEC03	EC_3626	2003	Ecuador		potato	Forbes	EC-1
PiEC06	EC_3841	2004	Ecuador		<i>S. habrochaites</i>	Forbes	US-1
PiEC07	EC_3921	2006	Ecuador		<i>S. jugandifolium</i>	Forbes	US-1
PiEC08	EC_3774	2004	Ecuador		<i>S. ochanthum</i>	Forbes	US-1
PiEC10	EC_3378	2001	Ecuador		<i>S. lycopersicum</i>	Forbes	US-1
PiEC11	EC_3381	2001	Ecuador		<i>S. lycopersicum</i>	Forbes	US-1
PiEC12	EC_3150	1997	Ecuador		<i>S. muricatum</i>	Forbes	US-1
PiEC13	EC_3520	2002	Ecuador		<i>S. muricatum</i>	Forbes	US-1
PiEC14	EC_3809	2004	Ecuador		<i>S. caripense</i>	Forbes	US-1
PiES01	2005_10	2005	Estonia		potato	Fry	
PiES02	2005_17	2005	Estonia		potato	Fry	
PiES03	2005_19	2004	Estonia		potato	Fry	
PiES04	2004_4	2004	Estonia		potato	Fry	
PiES05	2004_16	2004	Estonia		potato	Fry	
PiHU02	Josze_S32		Hungary		potato	Bakonyi	

PiMX03	MX980211	1998	Mexico		potato	Fry
PiMX04	MX980230	1998	Mexico		potato	Fry
PiMX05	MX980317	1998	Mexico		potato	Fry
PiMX06	MX980352	1998	Mexico		potato	Fry
PiMX07	MX980400	1998	Mexico		potato	Fry
PiMX10	PIC97008	1997	Mexico	Toluca	potato	Flier/Grünwald/PRI
PiMX11	PIC97066	1997	Mexico	Toluca	potato	Flier/Grünwald/PRI
PiMX12	PIC97106	1997	Mexico	Toluca	potato	Flier/Grünwald/PRI
PiMX13	PIC97111	1997	Mexico	Toluca	potato	Flier/Grünwald/PRI
PiMX14	PIC97130	1997	Mexico	Toluca	potato	Flier/Grünwald/PRI
PiMX15	PIC97136	1997	Mexico	Toluca	potato	Flier/Grünwald/PRI
PiMX16	PIC97146	1997	Mexico	Toluca	potato	Flier/Grünwald/PRI
PiMX17	PIC97149	1997	Mexico	Toluca	potato	Flier/Grünwald/PRI
PiMX18	PIC97153	1997	Mexico	Toluca	potato	Flier/Grünwald/PRI
PiMX19	PIC97159	1997	Mexico	Toluca	potato	Flier/Grünwald/PRI
PiMX20	PIC97187	1997	Mexico	Toluca	potato	Flier/Grünwald/PRI
PiMX21	PIC97310	1997	Mexico	Toluca	potato	Flier/Grünwald/PRI
PiMX22	PIC97318	1997	Mexico	Toluca	potato	Flier/Grünwald/PRI
PiMX23	PIC97335	1997	Mexico	Toluca	potato	Flier/Grünwald/PRI
PiMX24	PIC97340	1997	Mexico	Toluca	potato	Flier/Grünwald/PRI
PiMX25	PIC97389	1997	Mexico	Toluca	potato	Flier/Grünwald/PRI
PiMX26	PIC97392	1997	Mexico	Toluca	potato	Flier/Grünwald/PRI
PiMX27	PIC97423	1997	Mexico	Toluca	potato	Flier/Grünwald/PRI
PiMX28	PIC97432	1997	Mexico	Toluca	potato	Flier/Grünwald/PRI
PiMX29	PIC97438	1997	Mexico	Toluca	potato	Flier/Grünwald/PRI
PiMX30	PIC97442	1997	Mexico	Toluca	potato	Flier/Grünwald/PRI
PiMX40	PIC97716	1997	Mexico	Toluca	<i>S. demissum</i>	Flier/Grünwald/PRI
PiMX41	PIC97724	1997	Mexico	Toluca	<i>S. demissum</i>	Flier/Grünwald/PRI
PiMX42	PIC97727	1997	Mexico	Toluca	<i>S. demissum</i>	Flier/Grünwald/PRI
PiMX43	PIC97744	1997	Mexico	Toluca	<i>S. demissum</i>	Flier/Grünwald/PRI
PiMX44	PIC97748	1997	Mexico	Toluca	<i>S. demissum</i>	Flier/Grünwald/PRI

PiMX45	PIC97749	1997	Mexico	Toluca	<i>S. demissum</i>	Flier/Grünwald/PRI	
PiMX46	PIC97750	1997	Mexico	Toluca	<i>S. demissum</i>	Flier/Grünwald/PRI	
PiMX47	PIC97751	1997	Mexico	Toluca	<i>S. demissum</i>	Flier/Grünwald/PRI	
PiMX48	PIC97785	1997	Mexico	Toluca	<i>S. demissum</i>	Flier/Grünwald/PRI	
PiMX49	PIC97791	1997	Mexico	Toluca	<i>S. demissum</i>	Flier/Grünwald/PRI	
PiMX50	PIC97793	1997	Mexico	Toluca	<i>S. demissum</i>	Flier/Grünwald/PRI	
PiMX61	Tlax 701	2007	Mexico	Tlaxcala	potato	Fernández Pavia	
PiMX62	Tlax 715	2007	Mexico	Tlaxcala	potato	Fernández Pavia	
PiMX63	Tlax 722	2007	Mexico	Tlaxcala	potato	Fernández Pavia	
PiMX64	Tlax 728	2007	Mexico	Tlaxcala	potato	Fernández Pavia	
PiMX65	Tlax 740	2007	Mexico	Tlaxcala	potato	Fernández Pavia	
PiMX66	Tlax 748	2007	Mexico	Tlaxcala	potato	Fernández Pavia	
PiMX67	Tlax 756	2007	Mexico	Tlaxcala	potato	Fernández Pavia	
PiMX71	T48	2003	Mexico	Tlaxcala	potato	Fernández Pavia	
PiMX72	T68	2003	Mexico	Tlaxcala	potato	Fernández Pavia	
PiNL01	NL_01096	2001	Netherlands		potato	Kessel	
PiNL02	NL_96259	1996	Netherlands		potato	Kessel	
PiPE01	BTLM 004	1997	Peru	Lima	NA	Forbes	PE-7
PiPE02	PHU 076	2003	Peru	Huánuco	potato	Forbes	EC-1
PiPE03	PHU 079	2003	Peru	Huánuco	potato	Forbes	EC-1
PiPE04	PPI 015	2000	Peru	Piura	<i>S. huancabambense</i>	Forbes	EC-1
		1998					EC-1
PiPE05	PTS 031		Peru	Cajamarca	<i>S. caripense</i>	Forbes	
PiPE06	1696	1995	Peru	Arequipa	potato	Forbes	PE-3
PiPE07	PCA 004	1999	Peru	Cajamarca	potato	Forbes	PE-3
PiPE08	PCZ 024	1997	Peru	Cuzco	potato	Forbes	EC-1
PiPE09	PCZ 080	1997	Peru	Cuzco	potato	Forbes	EC-1
PiPE10	PSR 001	2005	Peru	Junín	NA	Forbes	EC-1
PiPE11	PCA 020	1999	Peru	Cajamarca	NA	Forbes	PE-7
PiPE12	PLI 003	1999	Peru	Lima	NA	Forbes	PE-7
PiPE13	PLI 036	2000	Peru	Lima	<i>S. wittmackii</i>	Forbes	PE-7

PiPE14	POX 100	2003	Peru	Pasco	potato	Forbes	PE-7
PiPE20	PCA 025	1999	Peru	Cajamarca	NA	Forbes	US-1
PiPE21	PPI 009	2000	Peru	Piura	<i>S. caripense</i>	Forbes	US-1
PiPE22	PPI 013	2000	Peru	Piura	<i>S. caripense</i>	Forbes	US-1
PiPE23	PPI 014	2000	Peru	Piura	<i>S. caripense</i>	Forbes	US-1
PiPE24	PPI 023	2000	Peru	Piura	<i>S. caripense</i>	Forbes	US-1
PiPE25	PPI 028	2000	Peru	Piura	<i>S. caripense</i>	Forbes	US-1
PiPE26	PPU 048	1997	Peru	Puno	potato	Forbes	PE-3
PiPE27	PPU 097	1997	Peru	Puno	potato	Forbes	US-1
PiPE28	PCA 006	1999	Peru	Cajamarca	potato	Forbes	PE-3
PiPE29	PCA 010	1999	Peru	Cajamarca	potato	Forbes	PE-3
PiPO01	MP_618	2005	Poland		potato	Lebecka	
PiPO02	MP_622	2005	Poland		potato	Lebecka	
PiSA01	SA960008	1996	South Africa		potato	Fry	US-1
PiSW01	SE_03058	2003	Sweden		potato	Andersson	
PiSW02	SE_03087	2003	Sweden		potato	Andersson	
PiUK01	2006_3984C	2006	UK		potato	Cooke	EU_1_A1
PiUK02	2006_4012F	2006	UK		potato	Cooke	EU_3_A2
PiUK03	2006_3928A	2006	UK		potato	Cooke	EU_13_A2
PiUK04	2006_4132B	2006	UK		potato	Cooke	EU_13_A2
PiUK05	2006_3888A	2006	UK		potato	Cooke	EU_2_A1
PiUK06	2007_5866B	2007	UK		potato	Cooke	EU_5_A1
PiUK07	2006_4388D	2006	UK		potato	Cooke	EU_17_A2
PiUK08	2006_4100A	2006	UK		potato	Cooke	EU_6_A1
PiUK09	2006_4440C	2006	UK		potato	Cooke	EU_10_A2
PiUK10	2006_4232E	2006	UK		potato	Cooke	EU_8_A1
PiUS08	US040009	2004	USA		potato	Fry	US-8
PiUS11	US050007	2005	USA		tomato	Fry	US-11
PiUS12	US940494	1994	USA		tomato	Fry	US-12
PiUS17	US970001	1997	USA		tomato	Fry	US-17
PiVT01	Vn02-076	2002	Vietnam		tomato	Le	US-1

PiVT02	Vn02-106	2002	Vietnam	tomato	Le	US-1
PiVT03	Vn03-416	2003	Vietnam	potato	Le	US-1
PiVT04	Vn03-590	2003	Vietnam	potato	Le	US-1
<i>P. mirabilis</i>						
PmMX01	CBS 136.86		Mexico	NA	CBS	
PmMX02	CBS 678.85		Mexico	NA	CBS	
PmMX03	DF 409		Mexico	NA	Fernández Pavia	
PmMX04	G 11-3	1998	Mexico	NA	Flier/Grünwald/PRI	
PmMX05	00M 410	2000	Mexico	NA	Fernández Pavia	
PmMX06	P 3001		Mexico	NA	Flier/Grünwald/PRI	
PmMX07	P 3006		Mexico	NA	Flier/Grünwald/PRI	
PmMX08	P mirabilis DF 07	2007	Mexico	NA	Fernández Pavia	
PmMX09	P. mirabilis Mich	2003	Mexico	NA	Fernández Pavia	
PmMX10	WF014/PIC99114	1999	Mexico	NA	Flier/Grünwald/PRI	
PmMX11	WF035/PIC99135	1999	Mexico	NA	Flier/Grünwald/PRI	
<i>P. ipomoeae</i>						
PoMX01	00Ip5	2000	Mexico	NA	Fernández Pavia	
PoMX02	Ipom1-2	1999	Mexico	NA	Flier/Grünwald/PRI	
PoMX03	Ipom2-1	1999	Mexico	NA	Flier/Grünwald/PRI	
PoMX04	Ipom2-4	1999	Mexico	NA	Flier/Grünwald/PRI	
PoMX05	Ipom3-3	1999	Mexico	NA	Flier/Grünwald/PRI	
PoMX06	Ipom6	1999	Mexico	NA	Flier/Grünwald/PRI	
PoMX07	P. ipomoeae	1999	Mexico	NA	Fernández Pavia	
<i>P. andina</i>						
PaEC01	EC_3189	1998	Ecuador	<i>Anarrichomenum</i>	Forbes	
PaEC02	EC_3399	2001	Ecuador	<i>Anarrichomenum</i>	Cooke	
PaEC03	EC_3818	2004	Ecuador	<i>Anarrichomenum</i>	Cooke	
PaEC04	EC_3821	2004	Ecuador	<i>Anarrichomenum</i>	Forbes	
PaEC05	EC_3780	2004	Ecuador	<i>S. hispidum</i>	Forbes	
PaEC06	EC_3655	2003	Ecuador	<i>S. hispidum</i>	Forbes	

PaEC07	EC_3163	1998	Ecuador	<i>Anarrichomenum</i>	Forbes
PaEC08	EC_3510	2002	Ecuador	<i>S. betaceum</i>	Forbes
PaEC09	EC_3540	2002	Ecuador	<i>Anarrichomenum</i>	Forbes
PaEC10	EC_3561	2002	Ecuador	<i>S. quitoense</i>	Forbes
PaEC11	EC_3563	2002	Ecuador	<i>S. quitoense</i>	Forbes
PaEC12	EC_3678	2003	Ecuador	<i>Anarrichomenum</i>	Forbes
PaEC13	EC_3836	2004	Ecuador	<i>S. betaceum</i>	Forbes
PaEC14	EC_3860	2005	Ecuador	<i>Torva</i>	Forbes
PaEC15	EC_3864	2005	Ecuador	<i>Torva</i>	Forbes
PaEC16	EC_3865	2005	Ecuador	<i>S. jugandifolium</i>	Forbes
PaEC17	EC_3936	2006	Ecuador	<i>S. ochanthum</i>	Forbes
PaPE01	POX 102	2003	Peru	<i>S. betaceum</i>	Forbes
PaPE02	POX 103	2003	Peru	<i>S. betaceum</i>	Forbes

P. phaseoli

PpUS01	CBS 556.88			CBS
PpUS02	P10150	USA	Delaware	Coffey

¹ Isolates were contributed by the authors and the following colleagues: Sampled by W. G. Flier and N. J. Grünwald and curated by Geert Kessel, Plant Research International (PRI), Netherlands; Geert Kessel, Plant Research International (PRI), Netherlands; Silvia Fernández Pavia, Universidad Michoacana de San Nicolás de Hidalgo, Mexico; Michael Coffey, University of California Riverside, USA; Vihn Hong Le and Arne Hermansen, Norwegian Institute for Agricultural and Environmental Research, Norway; Björn Andersson, Swedish University of Agricultural Sciences, Sweden; Renata Lebecka Młochow Research Centre, Poland; Jozsef Bakonyi, Academy of Agricultural Sciences, Hungary.

Table S2. Molecular clock and mutation rates obtained in this study for each locus for (A) Clade 1c and (B) *P. infestans* datasets. See Table S3 for indices of nucleotide variation at each locus.

A. Clade 1c

Locus	Clock	Clock Rate	UCLD stdev
β-tubulin	Strict	0.824	0.04
RAS	Log Normal	1.839	2.2
Trp1	Strict	1.73	0.03
PITG_11126	Strict	4.09	0.02

B. *P. infestans*

Locus	Clock	Clock Rate	UCLD stdev
β-tubulin	Strict	0.54	0.02
RAS	Log Normal	2.25	1.94
Trp1	Strict	1.73	0.012
PITG_11126	Strict	3.03	0.01

Table S3. Nucleotide variation by locus, species, and sampling location. Statistics given are number of individuals (N_{ind}), number of sequences (N_{seq}), length of alignment excluding gaps (L), segregating sites (S), number of heterozygous sites (Het), number of haplotypes (Hap), average pairwise nucleotide diversity (π), Watterson's theta (θ_w), Tajima's D, and Fu and Li's D* and F* (4-7).

Locus	Species/Popn	N_{ind}	N_{seq}	L	S	Het	Hap	π	θ_w	Tajima's D	Fu & Li's D*	Fu & Li's F*
PITG_11126												
	<i>P. infestans</i>	119	242	764	13	13 [#]	10	0.00286	2.144	0.04	0.79	0.61
	Europe	22	46	764	7	7 [#]	5	0.00294	1.593	1.10	1.25	1.41
	Mexico	48	96	764	9	9 [#]	6	0.00154	1.752	-0.82	-0.17	-0.47
	S. America	40	82	764	11	11 [#]	8	0.00394	2.210	0.97	0.79	1.01
	United States	4	8	779	2	2	2	0.00138	0.771	1.45	1.11	1.30
	Africa/Asia	5	10	779	3	3	2	0.00214	1.060	2.06*	1.15	1.53
	<i>P. andina</i>	19	38	748	16	16 [#]	3	0.01040	3.808	3.39***	1.58**	2.56**
	<i>P. ipomoeae</i>	7	14	787	2	1	3	0.00052	0.629	-0.96	-0.45	-0.66
	<i>P. mirabilis</i>	11	22	778	11	11	3	0.00593	4.610	1.83	1.44*	1.80**
	<i>P. phaseoli</i>	2	4	779	0	0	1	0	0	NA	NA	NA
β-tubulin												
	<i>P. infestans</i>	118	238	1590	9	9 [#]	8	0.00138	1.488	1.06	-0.43	0.13
	Europe	22	44	1590	6	6 [#]	3	0.00061	1.379	-0.79	1.18	0.67
	Mexico	48	96	1590	7	7 [#]	3	0.00185	1.363	2.75**	1.20	2.03**
	S. America	39	80	1590	9	9 [#]	7	0.00113	1.817	-0.03	-0.84	-0.67
	United States	4	8	1590	5	5 [#]	3	0.00124	1.928	0.08	0.75	0.65
	Africa/Asia	5	10	1590	0	0	1	0	0	NA	NA	NA
	<i>P. andina</i>	19	38	1590	23	23	2	0.00743	5.474	3.92***	1.70**	2.89**
	<i>P. ipomoeae</i>	7	14	1590	2	2	2	0.00018	0.629	-1.48	-1.83	-1.97
	<i>P. mirabilis</i>	11	22	1590	16	15 [#]	6	0.00469	4.389	2.54**	1.54**	2.14**
	<i>P. phaseoli</i>	2	4	1590	0	0	1	0	0	NA	NA	NA
Trp1												
	<i>P. infestans</i>	117	234	813	9	7	9	0.00183	1.492	-0.004	0.42	0.32
	Europe	22	44	813	4	3	4	0.00185	0.920	1.48	-0.06	0.47
	Mexico	48	96	813	6	4	5	0.00144	1.168	-0.20	1.12	0.81
	S. America	38	76	813	6	6	6	0.00211	1.224	0.95	0.22	0.54
	United States	4	8	813	4	4	4	0.00180	1.543	-0.22	-0.18	-0.21
	Africa/Asia	5	10	813	3	3	2	0.00205	1.060	2.06*	1.15	1.53
	<i>P. andina</i>	19	38	813	10	10	3	0.00293	2.380	3.48***	1.40*	2.42**
	<i>P. ipomoeae</i>	7	14	812	0	0	1	0	0	NA	NA	NA
	<i>P. mirabilis</i>	11	22	813	1	1	2	0.00011	0.274	-1.16	-1.57	-1.68
	<i>P. phaseoli</i>	2	4	813	0	0	1	0	0	NA	NA	NA
RAS												
	<i>P. infestans</i>	117	234	762	15	15 [#]	13	0.00364	2.487	0.290	0.311	0.364
	Europe	21	42	766	10	10	6	0.00569	2.324	2.585*	1.40	2.096**
	Mexico	47	94	766	11	11 [#]	8	0.00164	2.150	-1.09	-2.51*	-2.39*
	S. America	40	80	762	10	10	5	0.00377	2.019	1.12	1.38	1.53
	United States	4	8	766	11	11	4	0.00643	4.242	0.808	1.52**	1.50
	Africa/Asia	5	10	766	1	1	2	0.00205	1.060	2.06*	1.15	1.53
	<i>P. andina</i>	17	34	765	23	23 [#]	4	0.01433	5.625	3.28***	1.39	2.37**
	<i>P. ipomoeae</i>	7	14	768	3	0	2	0.00103	0.943	-0.49	1.07	0.76
	<i>P. mirabilis</i>	10	20	766	6	6 [#]	3	0.00091	1.973	-2.13*	-3.08**	-3.25**
	<i>P. phaseoli</i>	1	2	764	0	0	1	0	0	NA	NA	NA

[#]Also heterozygous for one or more indel.

* P < 0.05

** P < 0.02

*** P < 0.001

Table S4. Results from testing relationships among Toluca population, US1 and Andean lineages as illustrated in Figure S10.

Andean lineage	Scenario	Admixed population	Probability	95% CI
PE3	1	-	0.0040	[0.0028,0.0052]
	2	-	0.0071	[0.0058,0.0084]
	3	-	0.0066	[0.0055,0.0077]
	4	PE3	0.0014	[0.0010,0.0017]
	5	Toluca	0.0062	[0.0051,0.0073]
	6	US1	0.0009	[0.0008,0.0011]
	7	PE3	0.6709	[0.6478,0.6939]
	8	PE3	0.1094	[0.0994,0.1194]
	9	US1	0.0023	[0.0011,0.0034]
	10	US1	0.0052	[0.0034,0.0070]
	11	Toluca	0.0020	[0.0009,0.0032]
	12	Toluca	0.1302	[0.1093,0.1511]
	13	PE3	0.0474	[0.0410,0.0537]
	14	US1	0.0011	[0.0004,0.0017]
	15	Toluca	0.0053	[0.0034,0.0073]
PE7	1	-	0.0089	[0.0055,0.0124]
	2	-	0.0327	[0.0265,0.0389]
	3	-	0.0141	[0.0107,0.0176]
	4	PE7	0.0038	[0.0025,0.0051]
	5	Toluca	0.0093	[0.0073,0.0112]
	6	US1	0.0191	[0.0148,0.0234]
	7	PE7	0.3656	[0.3393,0.3919]
	8	PE7	0.2893	[0.2656,0.3131]
	9	US1	0.0016	[0.0003,0.0030]
	10	US1	0.0248	[0.0145,0.0350]
	11	Toluca	0.0121	[0.0032,0.0211]
	12	Toluca	0.0880	[0.0673,0.1087]
	13	PE7	0.1242	[0.1069,0.1416]
	14	US1	0.0012	[0.0003,0.0022]
	15	Toluca	0.0050	[0.0021,0.0079]
EC1	1	-	0.2524	[0.2335,0.2713]
	2	-	0.0293	[0.0260,0.0326]
	3	-	0.0575	[0.0519,0.0631]
	4	EC1	0.0908	[0.0830,0.0987]
	5	Toluca	0.0843	[0.0773,0.0913]
	6	US1	0.0216	[0.0192,0.0239]
	7	EC1	0.0320	[0.0276,0.0364]
	8	EC1	0.3060	[0.2811,0.3309]
	9	US1	0.0071	[0.0053,0.0088]
	10	US1	0.0234	[0.0188,0.0280]
	11	Toluca	0.0177	[0.0144,0.0210]
	12	Toluca	0.0140	[0.0116,0.0163]
	13	EC1	0.0088	[0.0069,0.0106]
	14	US1	0.0517	[0.0420,0.0614]
	15	Toluca	0.0035	[0.0026,0.0043]

Table S5. Nucleotide substitution model for each locus as inferred from jModelTest and ModelGenerator. The appropriate most similar model available in BEAST was used for each analysis.

A. Clade 1c

Locus	jModelTest	ModelGenerator	Model Used
β-tubulin	HKY	HKY	HKY
RAS	JC	JC	JC
Trp1	K80	HKY	HKY
PITG_11126	HKY	HKY	HKY

B. *P. infestans*

Locus	jModelTest	ModelGenerator	Model Used
β-tubulin	HKY	HKY	HKY
RAS	F81	JC	JC
Trp1	HKY	HKY	HKY
PITG_11126	HKY	HKY	HKY

Table S6. Settings used for DIYABC analyses. All runs used the same summary statistics: within population statistics were number of segregating sites, mean of pairwise differences, variance of pairwise differences, and number of private segregating sites; between population statistics were number of segregating sites, mean of pairwise differences, and F_{ST} . Posterior probabilities of scenarios were calculated using the closest 1% of simulated datasets using logistic regression.

A. Prior distributions for scenarios in Figure S9.

Parameter	Shape	Min.–Max.	Increment
Population size			
EC-1	Uniform	1–200000	1
PE-3	Uniform	1–200000	1
PE-7	Uniform	1–200000	1
Ancestor of two lineages	Uniform	1–500000	1
Ancestor of three lineages	Uniform	1–1000000	1
Time since divergence¹			
t1: two lineages	Uniform	1–300000	1
t2: all three lineages	Uniform	1–500000	1
Nucleotide sequence evolution²			
Mean mutation rate	Uniform	$1.00 \times 10^{-10} – 1.00 \times 10^{-8}$	
Gamma distribution	Uniform	$1.00 \times 10^{-11} – 1.00 \times 10^{-7}$	2.00

¹ An additional condition was put on the prior distributions such that $t2 > t1$.

² The Kimura 2-parameter nucleotide substitution model was used with invariant sites=90 and gamma rate variation parameter $\alpha=0.050$.

B. Prior distributions for scenarios in Figure S10.

Parameter	Shape	Min.–Max.	Increment
Population size			
Toluca	Uniform	1–1000000	1
EC-1	Uniform	1–300000	1
PE-3	Uniform	1–200000	1
PE-7	Uniform	1–200000	1
US-1	Uniform	1–500000	1
Unsampled population	Uniform	1–2000000	1
Ancestor of two lineages	Uniform	1–2000000	1
Time since divergence³			
t1: two populations (scenarios 1-3)	Uniform	1–200000	1
t2: two or three populations	Uniform	1–500000	1
t3: sampled & unsampled populations (scenarios 7-15)	Uniform	1–10000000	1
Admixture events			
Proportion from parent population	Uniform	0.001–0.999	0.001
ta1: timing since admixture event (scenarios 4-12)	Uniform	1–300000	1
ta2: timing since admixture event (scenarios 13-15)	Uniform	1–1000000	1

Nucleotide sequence evolution⁴				
	Mean mutation rate	Uniform	$1.00 \times 10^{-10} - 1.00 \times 10^{-8}$	
	Gamma distribution	Uniform	$1.00 \times 10^{-11} - 1.00 \times 10^{-7}$	2.00

³ Additional conditions were put on the prior distributions to force the timing of events into the tree structure shown in Figure S9, including placing admixture events before or after population splits and ordering of the population splits such that t2>t1, t2>ta1, t3>ta1, ta2>t2, and t3>ta2.

⁴ The Kimura 2-parameter nucleotide substitution model was used with invariant sites=90 and gamma rate variation parameter $\alpha=0.050$.

C. Prior distributions for scenarios in Figure 5.

Parameter	Shape	Min.–Max.	Increment
Population size			
Toluca	Uniform	1–1000000	1
EC-1	Uniform	1–400000	1
PE-3	Uniform	1–200000	1
US-1	Uniform	1–400000	1
Unsampled population	Uniform	1–1000000	1
Ancestor to Toluca & EC-1	Uniform	10–1000000	1
Ancestor to Toluca & US-1	Uniform	10–1000000	1
Time since divergence⁵			
t1: Toluca–EC-1	Uniform	1–200000	1
t2: Toluca–US-1	Uniform	1–600000	1
t3: All populations	Uniform	1–1000000	1
Admixture events			
Proportion from parent population	Uniform	0.001–0.999	0.001
Timing since admixture event	Uniform	1–200000	1
Nucleotide sequence evolution⁶			
	Uniform	$1.00 \times 10^{-10} - 1.00 \times 10^{-8}$	
	Uniform	$1.00 \times 10^{-11} - 1.00 \times 10^{-7}$	2.00

⁵ Additional conditions were put on the prior distributions to force the timing of events into the tree structure shown in Figure 5, including placing admixture events before or after population splits and ordering of the population splits such that t3>t1, t3>t2.

⁶ The Kimura 2-parameter nucleotide substitution model was used with invariant sites=90 and gamma rate variation parameter $\alpha=0.050$.

Table S7. Inferred root subpopulation using three starting seeds for (A) the mitochondrial P3 and P4 regions using only isolates from Mexico and the Andes, and (B) the nuclear RAS locus, using the data from Gómez-Alpizar *et al.* (1).

A. P3 and P4

Theta	Migration	Seed 1		Seed 2		Seed 3	
		Root location	Prob.	Root location	Prob.	Root location	Prob.
1.8	0.3, 0.3	Mexico	0.505	Mexico	0.500	Andes	0.501
	1.0, 1.0	Andes	0.501	Andes	0.505	Mexico	0.508
	5.0, 5.0	Mexico	0.559	Mexico	0.556	Mexico	0.510
	10.0, 10.0	Mexico	0.587	Mexico	0.577	Andes	0.669
2.0	1.0, 1.0	Andes	0.504	Andes	0.501	Mexico	0.503
	5.0, 5.0	Andes	0.513	Andes	0.531	Andes	0.562
	10.0, 10.0	Andes	0.689	Mexico	0.727	Andes	0.549

B. RAS

Theta	Migration	Seed 1		Seed 2		Seed 3	
		Root location	Prob.	Root location	Prob.	Root location	Prob.
2.0	0.5, 0.5	SA	0.515	NSA	0.537	SA	0.535
	5.0, 5.0	SA	0.514	SA	0.582	SA	0.847
	10.0, 10.0	NSA	0.889	NSA	0.875	SA	0.686
	5.0, 10.0	SA	0.916	SA	0.949	SA	0.985
	10.0, 5.0	NSA	0.679	NSA	0.902	SA	0.935
	4.3, 14.6 *	SA	0.965	SA	0.992	SA	0.970
	14.6, 4.3	NSA	0.939	NSA	0.996	NSA	0.979

* Migration rates used by Gómez-Alpizar *et al.* (1)

Table S8. Root population inferred using RAS sequences from Mexico and Andean samples from this study. Migration rates were symmetric for all runs.

Simulations	Seed 1		Seed 2		Seed 3		Seed 4		
	θ	M	Root	Prob.	Root	Prob.	Root	Prob.	
			1×10^6		1×10^6		1×10^7		
1.5	0.5	Mexico	0.541	Mexico	0.584	Andes	0.510	Mexico	0.521
	5.0	Mexico	0.638	Mexico	0.703	Mexico	0.564	Mexico	0.583
	10.0	Andes	0.723	Mexico	0.975	Mexico	0.612	Andes	0.794
2.0	0.5	Andes	0.676	Andes	0.638	Mexico	0.513	Mexico	0.514
	5.0	Mexico	0.883	Andes	0.614	Mexico	0.590	Andes	0.794
	10.0	Mexico	0.714	Andes	0.688	Mexico	0.663	Mexico	0.939

Supporting Figures

Figure S1. Structure plots for K from 2 to 10 for the Andes (with and without admixture) and Mexico samples of *P. infestans*.

Figure S2. Delta K values obtained from Structure Harvester for (A) Mexico and (B) Andes (with admixture) samples of *P. infestans*. Note the highest delta K value corresponds to K=4 for Mexico and K=2 for the Andes.

Figure S3. Root state posterior probabilities for each location for (A) Clade 1c and (B) *P. infestans*. Independent analysis of each locus produced high probabilities for the root of both Clade 1c and *P. infestans* in Mexico (green bar).

Figure S4. Maximum clade credibility genealogy for the **β-tubulin** locus. Colors of branches indicate the most probable geographic origin of each lineage.

Figure S5. Maximum clade credibility genealogy for the **PITG_11126** locus. Colors of branches indicate the most probable geographic origin of each lineage.

Figure S6. Maximum clade credibility genealogy for the **RAS** locus. Colors of branches indicate the most probable geographic origin of each lineage.

Figure S7. Maximum clade credibility genealogy for the **Trp1** locus. Colors of branches indicate the most probable geographic origin of each lineage.

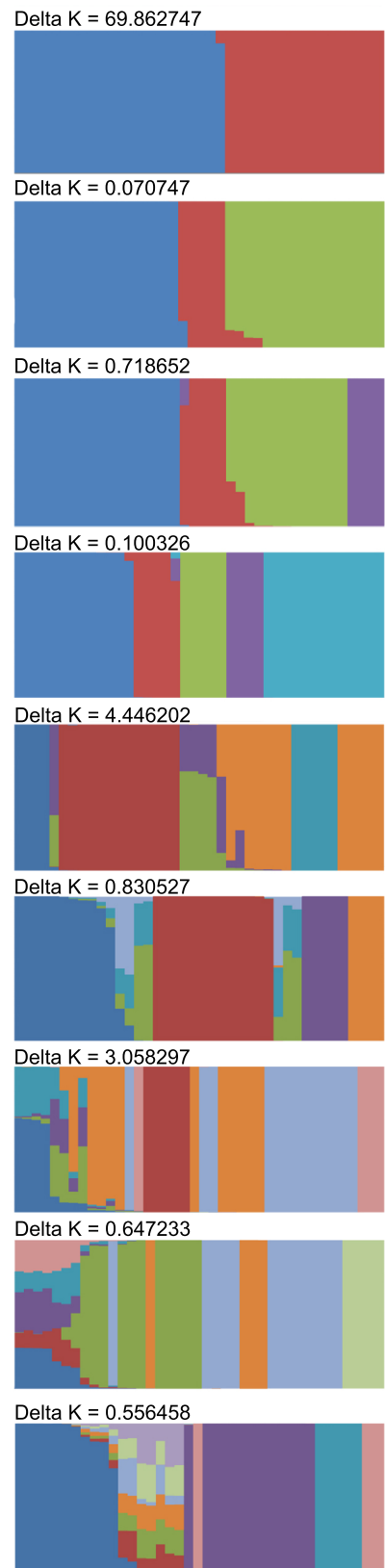
Figure S8. Maximum clade credibility phylogeny of *Phytophthora* Clade 1c from all four loci. Colors of branches indicate the most probable geographic origin of each lineage and taxon colors represent species (purple: *P. phaseoli*; blue: *P. ipomoeae*; green: *P. mirabilis*; red: *P. andina*; black: *P. infestans*).

Figure S9. Scenarios used to test evolutionary relationships among Andes lineages EC-1, PE-3, and PE-7 using DIYABC. Present day populations are at the base of the tree schematic. Ancestral relationships among these populations are represented by lines intersecting in the past, with the vertex of the schematic representing the most recent common ancestor of all samples. Horizontal lines indicate admixture events between the ancestral populations connected by the horizontal line. Change in line thickness indicates a potential change in population size, such that all branches in scenarios D, E, and F had independently estimated population sizes. The scenarios in which PE-3 and PE-7 diverged more recently from each other than from EC-1 produced high posterior probabilities.

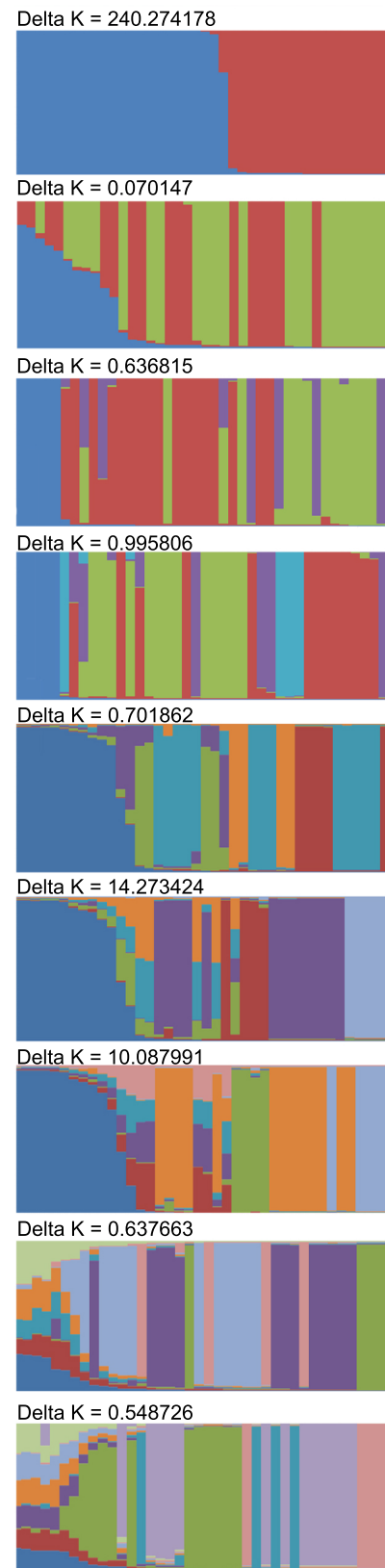
Figure S10. Scenarios used to test evolutionary relationships of EC-1, PE-3, and PE-7 lineages to US-1 in the Andes and to the Toluca, Mexico population. The 15 scenarios were compared against each other, using three independent sets of scenarios with EC-1, PE-3, and PE-7, in turn, substituted for population ‘X’. Present day populations are at the base of the tree schematic. Ancestral relationships among these populations are represented by lines intersecting in the past, with the vertex of the schematic representing the most recent common ancestor of all samples.

Horizontal lines indicate admixture events between the ancestral populations connected by the horizontal line. Potential changes in population size over time are indicated by changes in line thickness, but line thickness is not proportional to population size. The dashed line represents an unsampled population that has contributed to the genetic variation observed in sampled populations.

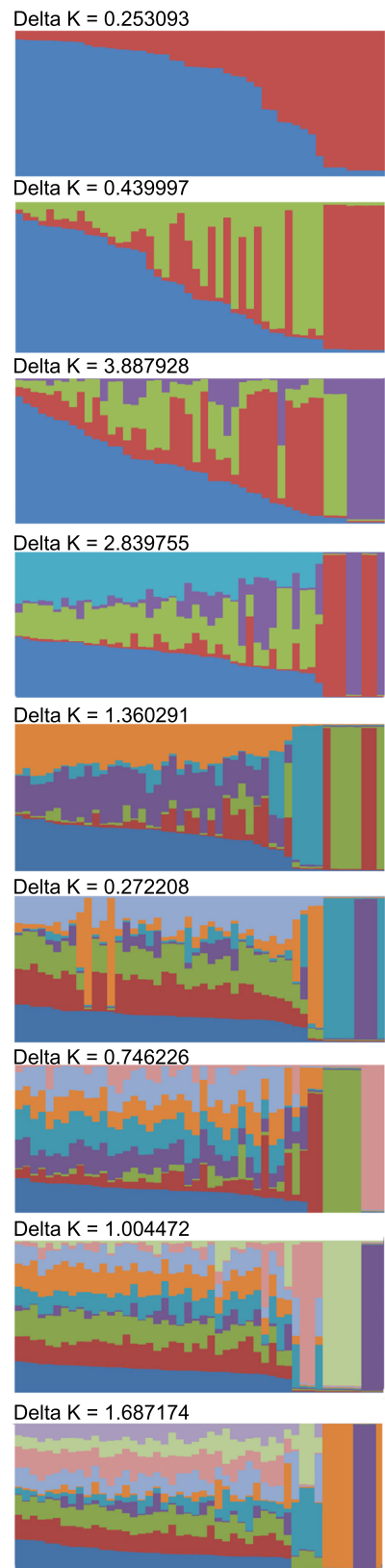
A. Andes (No admixture model)



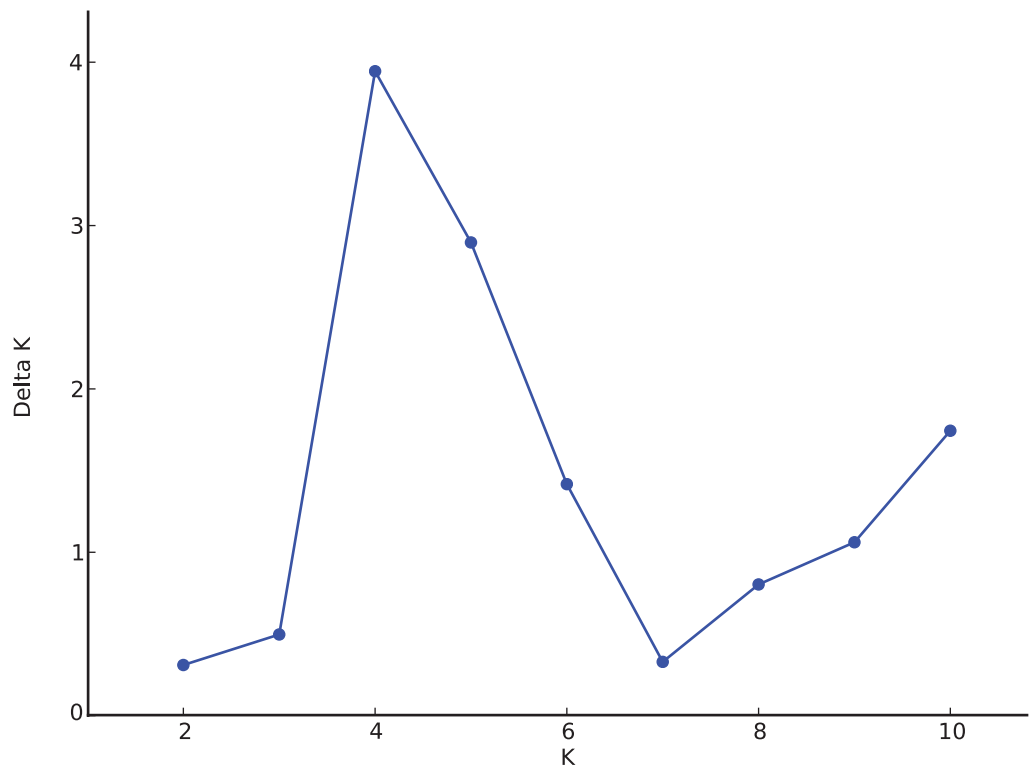
B. Andes (Admixture model)



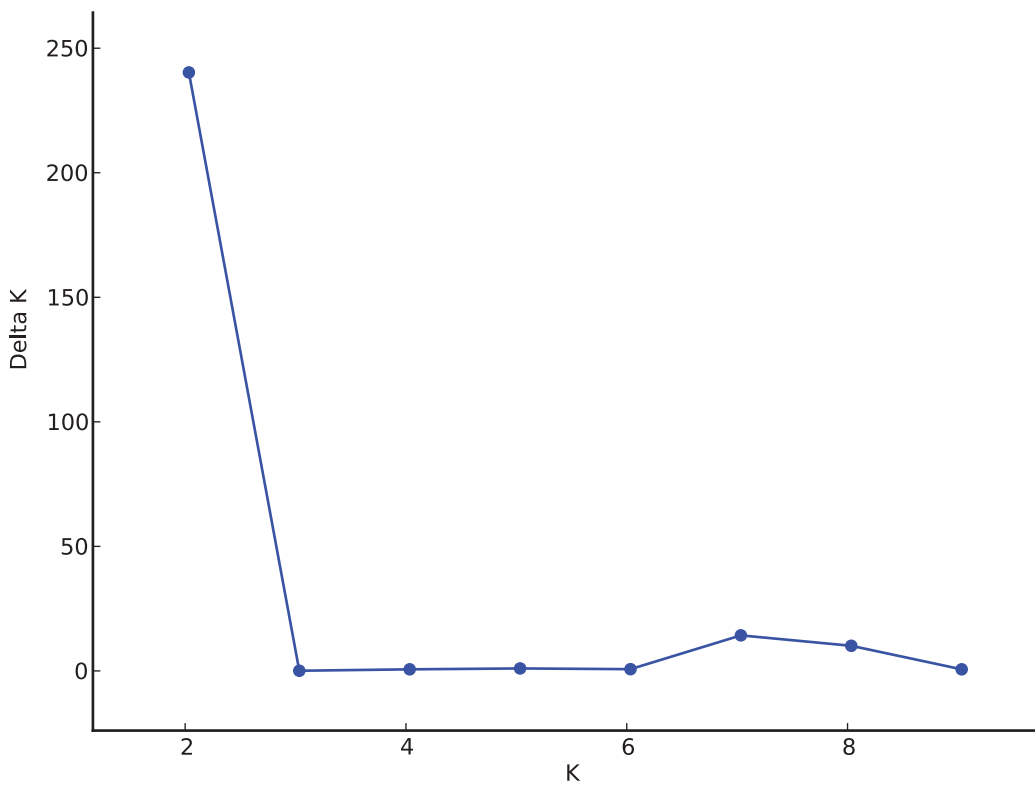
C. Mexico (Admixture model)



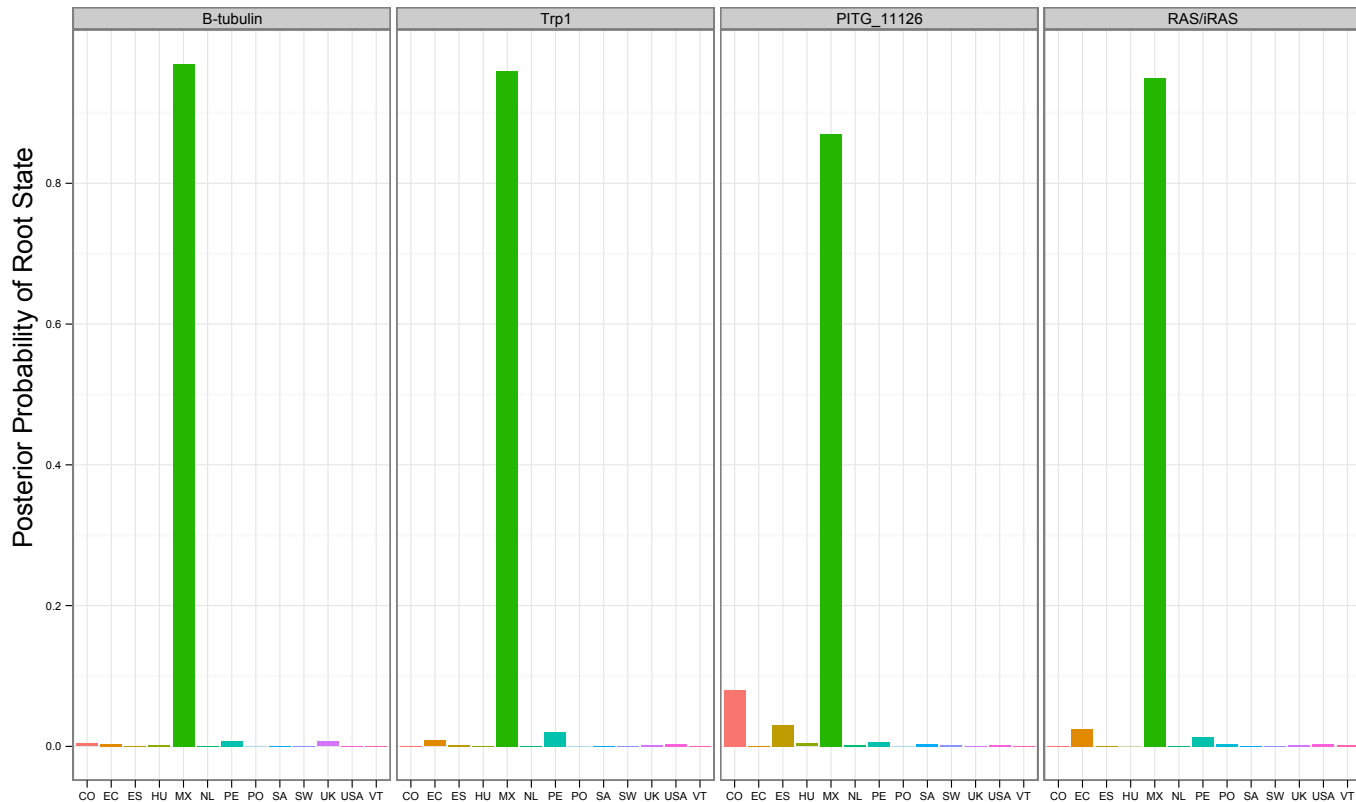
A. Mexico



B. Andes



A) Clade 1c



B) *P. infestans*

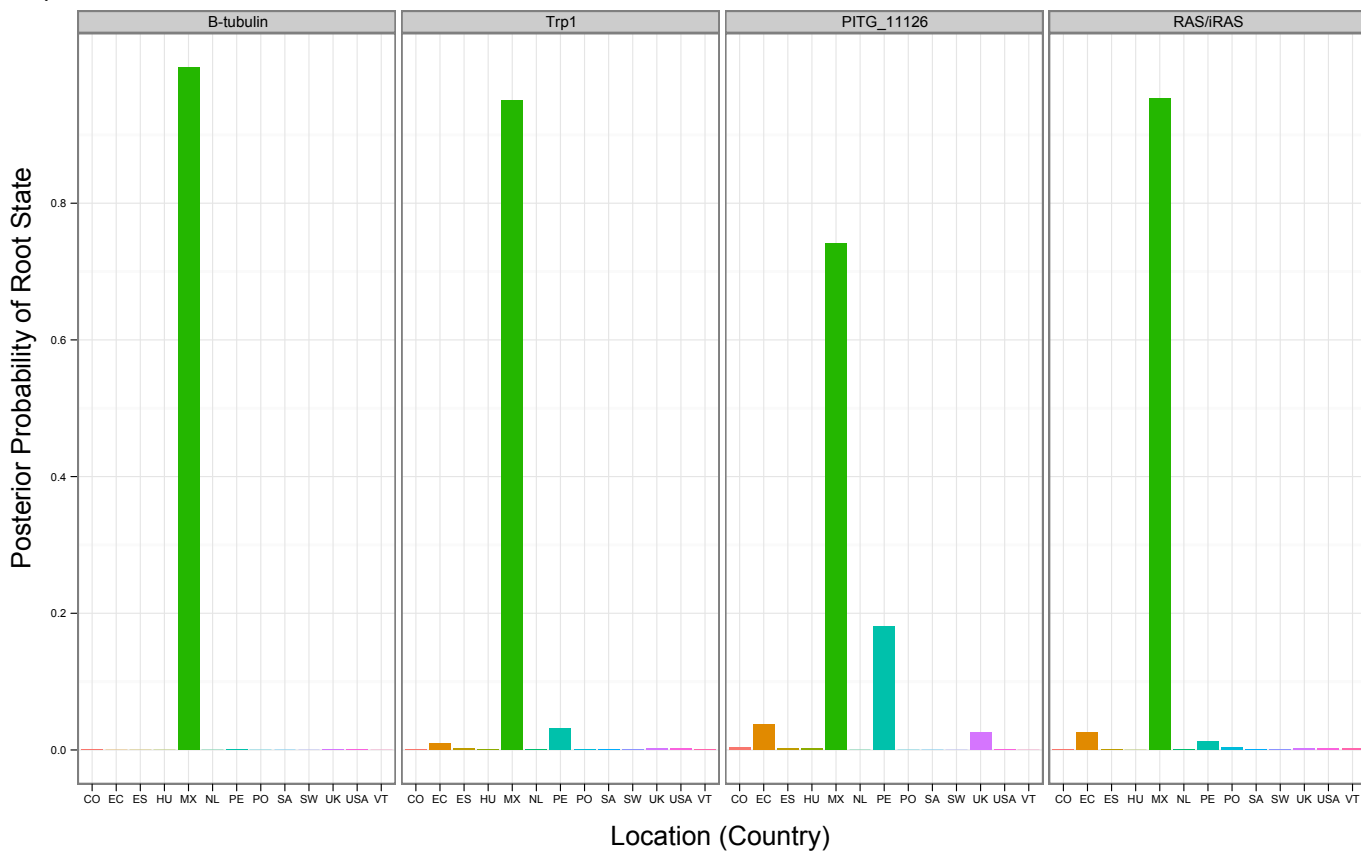


Figure S3. Root state posterior probability values for each location after 300 millions MCMC generations by locus for (A) Clade 1c species and (B) *P. infestans*. The posterior probability for a Mexico root (green bar) is higher than for any of the other countries for each locus independently and both datasets.

Figure S4. Maximum clade credibility genealogy for the **β -tubulin** locus. Colors of branches indicate the most probable geographic origin of each lineage.

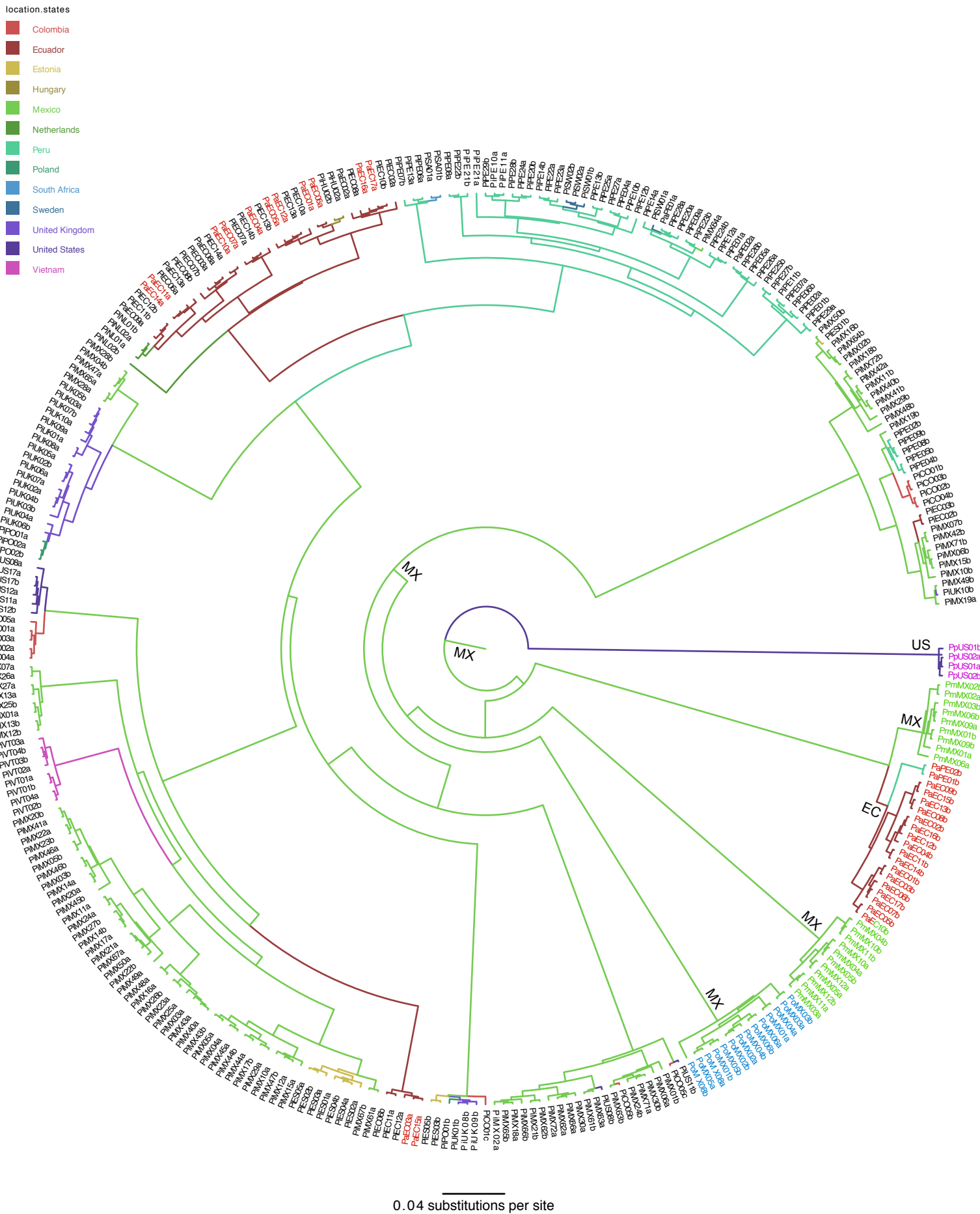


Figure S5. Maximum clade credibility genealogy for the **PITG_11126** locus. Colors of branches indicate the most probable geographic origin of each lineage.

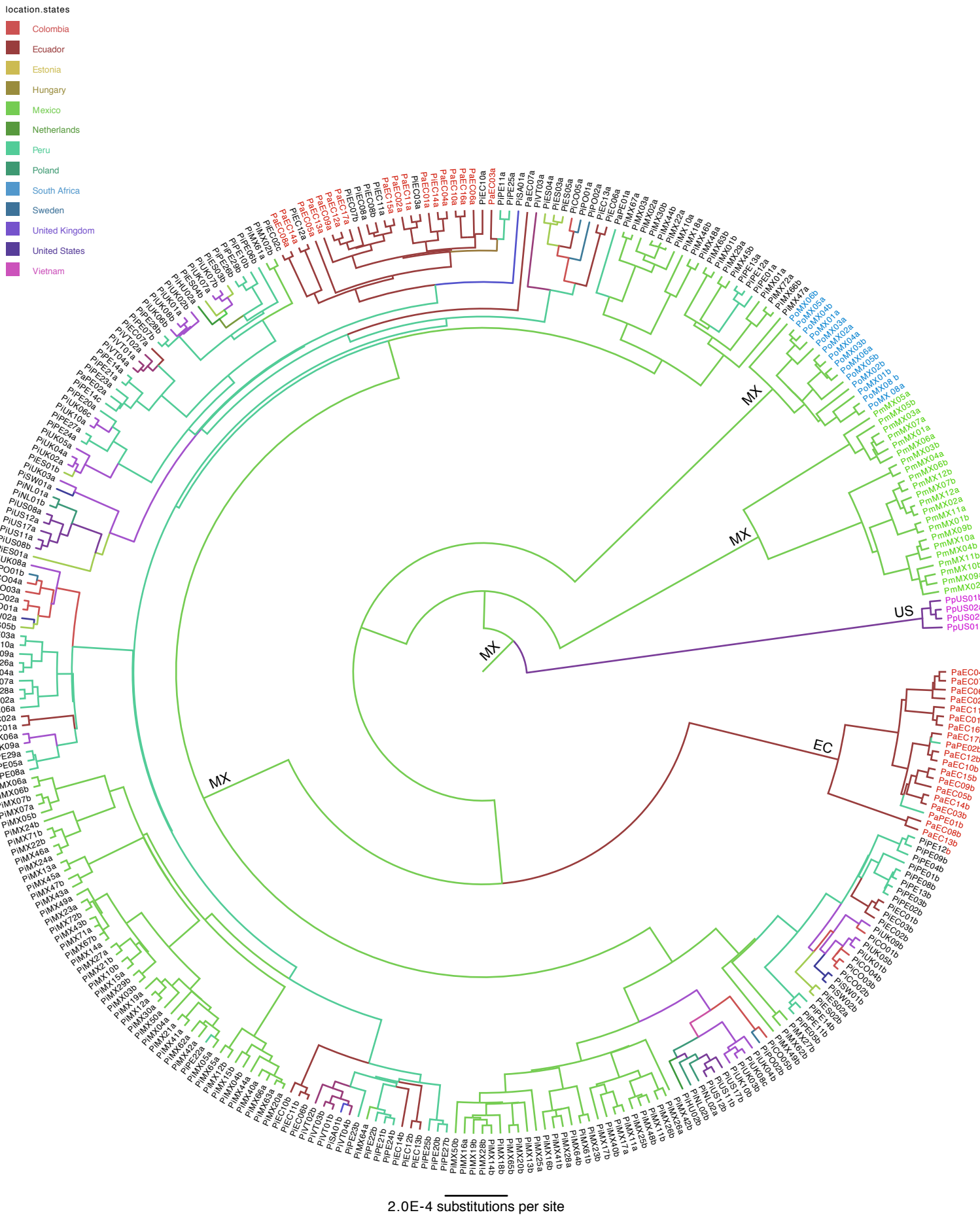


Figure S6. Maximum clade credibility genealogy for the RAS locus. Colors of branches indicate the most probable geographic origin of each lineage.

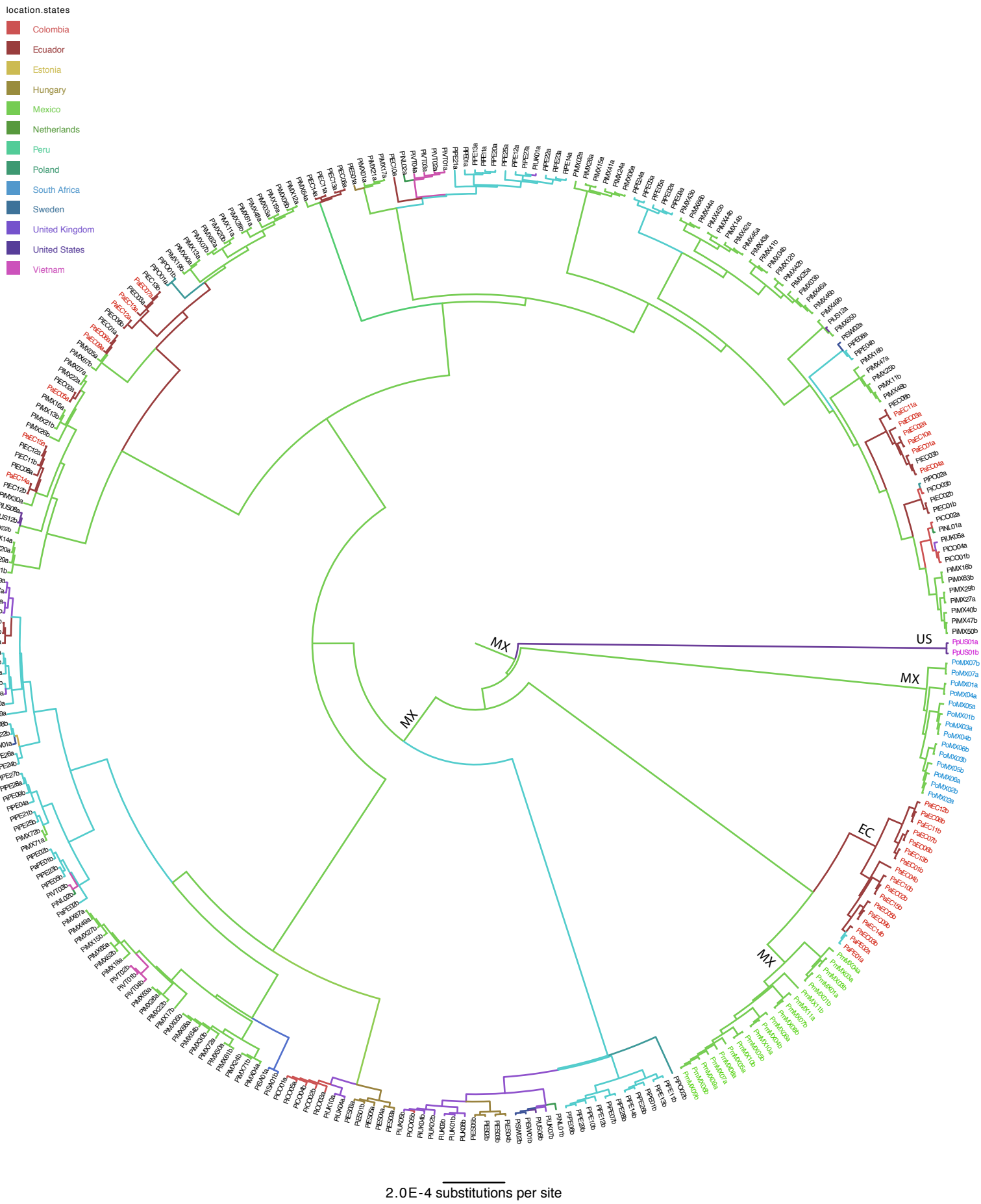


Figure S7. Maximum clade credibility genealogy for the **Trp1** locus. Colors of branches indicate the most probable geographic origin of each lineage.

